Adaptive Attitude Control of a Quadrotor Using Fast Nonsingular Terminal Sliding Mode

Shikang Lian, Wei Meng [ID], *Member, IEEE*, Zemin Lin, Ke Shao [ID],
Jinchuan Zheng [ID], *Senior Member, IEEE*, Hongyi Li [ID], *Senior Member, IEEE*,
and Renquan Lu [ID], *Senior Member, IEEE*

Abstract—As one type of unmanned aerial vehicles, the quadrotor typically suffers from payload variations, system uncertainties, and environmental wind disturbances, which significantly deteriorate its attitude control performance. To provide high-speed, accurate, and robust attitude tracking performance for the quadrotor, an adaptive fast nonsingular terminal sliding mode (AFNTSM) controller is proposed in this article. The proposed AFNTSM controller combines the advantages of fast nonsingular terminal sliding mode (FNTSM), integral sliding mode, and adaptive estimation techniques, which are effective to achieve the desired tracking performance and suppress control signal chattering. Furthermore, unlike conventional methods, the adaptive estimation removes the requirements for the upper bound information of the disturbances. It is proved that the proposed AFNTSM can guarantee finite-time convergence and zero tracking error for the quadrotor attitude control. Finally, comparative study with the FNTSM control only and conventional sliding mode control is conducted through experiments and the results demonstrate that the proposed AFNTSM can achieve faster convergence and stronger robustness in line with theoretical analysis.

Index Terms—Adaptive control, attitude control, quadrotor, sliding mode control, unmanned aerial vehicles.

I. INTRODUCTION

RECENTLY, owing to the advantages of small fuselage, sufficient power, and flexibility, quadrotors have been widely used in many civilian fields such as environmental detection [1]–[3], power line inspection [4], and plant protection in agriculture fields [5]. The attitude control is the basis for quadrotors to perform the tasks including trajectory tracking, attitude stabilization, etc., which is critical to satisfy high-performance mission requirements [6], [7]. The attitude controller of quadrotors is usually designed to be an underactuated subsystem owing to the high nonlinearity characteristics associated with the inherent unmodeled dynamics, parameter perturbation, and external disturbance [8], [9]. Thus far, a variety of robust controllers for attitude control have been investigated to achieve desired control performance, such as H_∞-based control [10], super twisting algorithm control [11], sliding mode control [12], integral backstepping control [13], and optimal control [14].

Sliding mode control (SMC) is well known for the properties of strong robustness and fast convergence rate. It is widely used in many applications such as robotic manipulators [15], linear motor positioners [16], underwater robots [17], etc. A backstepping-based approach combined with conventional sliding mode (CSM) control is presented in [18]. CSM control is presented for a class of underactuated systems in [19]. However, the CSM control can only guarantee the system asymptotic convergence to zero, which cannot satisfy the increasing requirements for swift response in quadrotor attitude control. To overcome this problem, terminal sliding mode control (TSM) is proposed in [15], which can drive the tracking error to zero by a nonlinear hyperplane. Nevertheless, the control input in conventional TSM control can produce boundless value when the system state is within a small neighborhood around zero. To avoid the possible control input singularity associated with the conventional TSM, a novel concept of nonsingular terminal sliding mode (NTSM) control is proposed in [20]. However, the frozen control gain of the discontinuous reaching control component in CSM and NTSM will lead to severe chattering, which may cause control input saturation or even damage the motors of the quadrotor. To reduce the control signal chattering of quadrotor, a series of strategies have been investigated such as second order sliding mode [21], fractional order sliding mode [22], and adaptive SMC [23]. Besides, a fast nonsingular terminal sliding mode (FNTSM) is developed in [24] for linear motor control systems

to eliminate the chattering by containing no switching element in the reaching control law. However, this method has to sacrifice the tracking accuracy, which is not desired for quadrotor attitude control. To improve the control precision, a recursive integral terminal sliding mode is constructed in [25], which guarantees that the tracking error can converge to zero and cancel the system chattering by introducing an adaptive disturbance observer.

In most sliding mode-based attitude controllers for quadrotor, high-speed response, accurate tracking, and strong robustness have not yet been simultaneously achieved so far. More specific, the FNTSM [24] controller eliminates the control signal chattering but sacrifices the tracking accuracy. Integral terminal sliding mode control is introduced in [26] to improve the tracking accuracy but it still contains chattering. To improve control robustness, adaptive integral second order sliding mode is proposed in [22] to handle the uncertainty and external disturbance. However, this method suppresses the transient response speed of the system state, which is unacceptable for quadrotor that requires high maneuverability. Moreover, most of the aforementioned control methods lack experimental verification on real quadrotors.

Motivated by the aforementioned discussions, an adaptive fast nonsingular terminal sliding mode (AFNTSM) control method for the quadrotor attitude control is proposed in this article. First, this article presents a quadrotor dynamic model with parametric uncertainty. Second, the control design procedure of the AFNTSM and stability proof of the quadrotor attitude closed-loop control system are elaborated. Finally, both outdoor flight and indoor comparative experiments are carried out on a real quadrotor to test the advantages of the presented controller. The main contributions of the proposed AFNTSM control method are summarized as follows.

1) The proposed AFNTSM attitude control scheme employs a fast nonsingular terminal sliding function with integral element, which can effectively improve the tracking accuracy whilst maintain fast response speed.

2) An adaptive estimation law is embedded in the AFNTSM controller to update the control gain online in accordance with the time-varying disturbances. This enhancement also removes the requirement for the upper bound information of the disturbance *a priori* in the control synthesis.

3) Instead of using fixed values, dynamic regulation for the control parameters in the sliding mode function is proposed, which can ease the tuning procedure to obtain desired tracking performance with moderate control chattering.

4) Performance in terms of fast response, high accuracy, and strong robustness of the proposed AFNTSM is verified on a real quadrotor prototype by conducting both outdoor flight experiments and indoor comparative study.

This article is organized as follows. Section II presents the structure and the dynamic model of a quadrotor with parametric uncertainty. The design method of AFNTSM controller is described in Section III, where stability analysis and control parameters are discussed in details. In Section IV, experiments results are presented. Finally, Section V concludes this article.
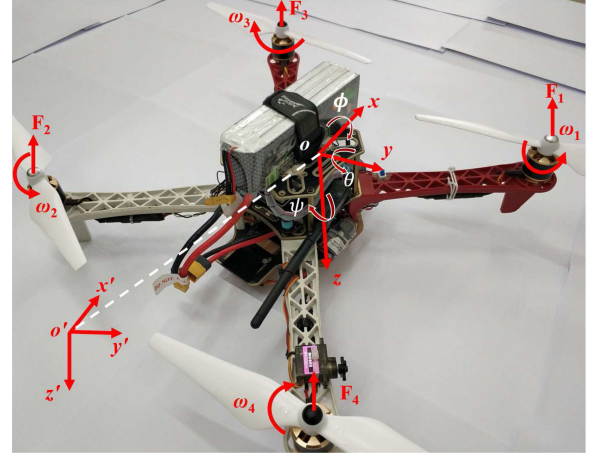

Fig. 1. Structure configuration of a quadrotor prototype.

II. PLANT MODELING

To obtain the mathematical model of the quadrotor, two basic coordinate systems are illustrated in Fig. 1, where $\mathbf{E}_G = o'\{x,'y,'z'\}$ denotes the inertial frame and $\mathbf{E}_B = o\{x, y, z\}$ denotes the body frame. The attitude of quadrotor is described by Euler angle $\mathbf{\Theta} = [\phi, \theta, \psi]^T$ in inertial frame $\mathbf{E}_G$ with each element denoting the roll, pitch and yaw angle around the x', y', and z' axis, respectively. The positive direction of attitude angle accords with right-hand rule. Furthermore, define the angular velocity of the aircraft body in body frame $\mathbf{E}_B$ as $\mathbf{\Omega}_b = [p, q, r]^T$. Then, the attitude rate $\dot{\mathbf{\Theta}}$ and the angular velocity of the aircraft body satisfy the following relationship:

$$\dot{\mathbf{\Theta}} = \mathbf{M}_b^g(\mathbf{\Theta})\mathbf{\Omega}_b \tag{1}$$

$$\mathbf{M}_b^g(\mathbf{\Theta}) = \begin{pmatrix} 1 & T_\theta S_\phi & T_\theta C_\phi \\ 0 & C_\phi & -S_\phi \\ 0 & S_\phi/C_\theta & C_\phi/C_\theta \end{pmatrix} \tag{2}$$

where $\mathbf{M}_b^g(\mathbf{\Theta})$ is a transformation matrix, which converts the attitude angular velocity of the quadrotor from body frame to inertial frame. In addition, the following notations are defined: $C_* := \cos(*)$, $S_* := \sin(*)$ and $T_* := \tan(*)$, $* \in \{\phi, \theta, \psi\}$. According to the principle of aerodynamics that the aerodynamic force and torque are proportional to the square of the propeller rotational speed, the lifting force and torque of the quadrotor can be described by the following equations:

$$\mathbf{F} = \sum_{i=1}^{4} F_i = k_t(\omega_1^2 + \omega_2^2 + \omega_3^2 + \omega_4^2)$$

$$\mathbf{M} = \begin{pmatrix} \tau_x \\ \tau_y \\ \tau_z \end{pmatrix} = \begin{pmatrix} \frac{\sqrt{2}}{2}l(-F_1 + F_2 + F_3 - F_4) \\ \frac{\sqrt{2}}{2}l(F_1 - F_2 + F_3 - F_4) \\ \frac{k_d}{k_t}(F_1 + F_2 - F_3 - F_4) \end{pmatrix}$$

$$= \begin{pmatrix} \frac{\sqrt{2}}{2}lk_t(-\omega_1^2 + \omega_2^2 + \omega_3^2 - \omega_4^2) \\ \frac{\sqrt{2}}{2}lk_t(\omega_1^2 - \omega_2^2 + \omega_3^2 - \omega_4^2) \\ k_d(\omega_1^2 + \omega_2^2 - \omega_3^2 - \omega_4^2) \end{pmatrix} \tag{3}$$

where $\mathbf{F}$ and $\mathbf{M}$ denote the aerodynamic force and torque generated by the four propellers with F_i the lifting force of each rotor and τ_* the $*$-direction torque acting on the quadrotor. l denotes the distance between the motor and the quadrotor center. k_t and k_d are the aerodynamic coefficients corresponding to the force and torque, respectively. ω_i denotes the spinning rate of the ith rotor on the quadrotor.

Based on the abovementioned analysis, the equation of motion of the quadrotor attitude model can be formulated by the following dynamic equations:

$$\begin{cases} \dot{\boldsymbol{\Theta}} = \mathbf{M}_b^g(\boldsymbol{\Theta})\boldsymbol{\Omega}_b \\ \mathbf{J}_b\dot{\boldsymbol{\Omega}}_b = -\boldsymbol{\Omega}_b \times (\mathbf{J}_b\boldsymbol{\Omega}_b) + \mathbf{G}_a + \mathbf{M} + \mathbf{f}_d + \mathbf{d} \end{cases} \quad (4)$$

where $\mathbf{J}_b$ denotes the moment of inertia of the quadrotor with respect to the body frame. Because of the symmetrical structure of the quadrotor, $\mathbf{J}_b = \text{diag}\{J_x, J_y, J_z\}$ is a diagonal matrix. $\mathbf{f}_d$ denotes air friction and $\mathbf{d} = [d_\phi, d_\theta, d_\psi]^T$ denotes external disturbance, both of which are assumed to be bounded. The $\mathbf{G}_a$ denotes gyroscopic moment. Under hovering condition, it is reasonable to apply small-angle approximations to (2) such that the trigonometric functions can be linearized. Hence, the equations in (4) can be approximated as

$$\ddot{\phi} = \ell_1^{-1}(\ell_2 qr + \tau_x - \ell_3\dot{\phi} + J_r q\widetilde{w} - d_\phi)$$

$$\ddot{\theta} = \ell_4^{-1}(\ell_5 pr + \tau_y - \ell_6\dot{\theta} - J_r p\widetilde{w} - d_\theta)$$

$$\ddot{\psi} = \ell_7^{-1}(\ell_8 pq + \tau_z - \ell_9\dot{\psi} - d_\psi) \quad (5)$$

where τ_x, τ_y, τ_z are the system control input to be designed

$$\ell_1 = J_x, \ell_2 = J_y - J_z, \ell_3 = \frac{\sqrt{2}k_f l}{2}$$

$$\ell_4 = J_y, \ell_5 = J_z - J_x, \ell_6 = \frac{\sqrt{2}k_f l}{2}$$

$$\ell_7 = J_z, \ell_8 = J_x - J_y, \ell_9 = k_f l \quad (6)$$

are inertia related constants and $\widetilde{w} = \omega_1 - \omega_2 + \omega_3 - \omega_4$. k_f denotes the coefficient of air resistance. J_r denotes the moment of inertia of the rotor.

In this article, we consider the following additive parameter uncertainties of the system model:

$$\ell_i = \ell_{i0} + \Delta\ell_i \quad (7)$$

where ℓ_{i0} $(i = 1, 2, \ldots, 9)$ represent the nominal values, and $\Delta\ell_i$ $(i = 1, 2, \ldots, 9)$ denote the corresponding uncertainties, respectively.

The control objective is to design a robust controller for $[\tau_x, \tau_y, \tau_z]^T$ such that fast and accurate attitude tracking performance can be guaranteed in the presence of uncertainties and disturbances. To further formulate this control problem, define the tracking error as

$$\begin{cases} e_\phi = \phi - \phi_d \\ e_\theta = \theta - \theta_d \\ e_\psi = \psi - \psi_d \end{cases} \quad (8)$$

where ϕ_d, θ_d, and ψ_d are the reference command supposed to be twice differentiable. Combining (8) with (5) and (7), the tracking

error dynamic equations are given by

$$\begin{cases} \ell_{10}\ddot{e}_\phi = \ell_{20}qr + \tau_x - \ell_{30}\dot{\phi} - \ell_{10}\ddot{\phi}_d - \delta_\phi \\ \ell_{40}\ddot{e}_\theta = \ell_{50}pr + \tau_y - \ell_{60}\dot{\theta} - \ell_{40}\ddot{\theta}_d - \delta_\theta \\ \ell_{70}\ddot{e}_\psi = \ell_{80}pq + \tau_z - \ell_{90}\dot{\psi} - \ell_{70}\ddot{\psi}_d - \delta_\psi \end{cases} \quad (9)$$

where $\delta_\phi = \Delta\ell_1\ddot{\phi} - \Delta\ell_2 qr + \Delta\ell_3\dot{\phi} - J_r q\widetilde{w} + d_\phi$, $\delta_\theta = \Delta\ell_4\ddot{\theta} - \Delta\ell_5 pr + \Delta\ell_6\dot{\theta} + J_r q\widetilde{w} + d_\theta$, and $\delta_\psi = \Delta\ell_7\ddot{\psi} - \Delta\ell_8 pq + \Delta\ell_9\dot{\psi} + d_\psi$ represent the lumped uncertainty of system (9), respectively. In addition, it is assumed that the lumped uncertainty satisfies

$$\begin{cases} |\frac{1}{\ell_{10}}\delta_\phi| < C_{\phi 1} + C_{\phi 2}|\phi| + C_{\phi 3}|\dot{\phi}| \\ |\frac{1}{\ell_{40}}\delta_\theta| < C_{\theta 1} + C_{\theta 2}|\theta| + C_{\theta 3}|\dot{\theta}| \\ |\frac{1}{\ell_{70}}\delta_\psi| < C_{\psi 1} + C_{\psi 2}|\psi| + C_{\psi 3}|\dot{\psi}| \end{cases} \quad (10)$$

where C_{*1}, C_{*2}, and C_{*3} are unknown but bounded positive number. This assumption has practical meaning. The first term C_{*1} on the right-hand side of (10) denotes uncertain time-invariant disturbances such as center of gravity shift or applied disturbance torque. The second term $C_{*2}|*|$ denotes uncertain torque due to mechanical stiffness and coupling of the attitude angle. The third term $C_{*3}|*|$ denotes uncertain torque due to unmodeled gyroscopic moment of four rotors $* \in \{\phi, \theta, \psi\}$.

III. CONTROLLER DESIGN

In this section, a robust attitude controller will be designed to guarantee the quadrotor system can track a reference command fast and accurately in the presence of the model uncertainties and disturbances. To achieve this goal, an integral terminal sliding function is introduced, based on which the steady-state error is eliminated and the finite-time convergence is achieved. Furthermore, to compensate for parametric uncertainties and unknown external disturbances, an online adaptive estimation law is embedded into the controller. Finally, selections of the control parameters are discussed.

A. AFNTSM for Quadrotor Attitude Control

According to [10], the coupling between the roll and pitch motion is negligible because the roll angle is nearly independent of the pitch angle if the variations of the reference command frequency and amplitude are less than 15 Hz and 25°. Thus, we simply consider the coupling as unmodeled system uncertainty that will be compensated by the proposed controller. Since the roll, pitch, and yaw motion have very similar dynamics, we only proceed the controller design for the roll motion for illustration.

To design the AFNTSM controller, the following integral terminal sliding mode function σ_ϕ is first defined

$$\sigma_\phi = \dot{e}_\phi + \int_{t_0}^t \lambda_{\phi 1}\text{sig}(e_\phi)^{\gamma_{\phi 1}} + \lambda_{\phi 2}\text{sig}(\dot{e}_\phi)^{\gamma_{\phi 2}}d\tau \quad (11)$$

where $\lambda_{\phi 1}$ and $\lambda_{\phi 2}$ are the positive control parameters to be designed. In addition, to ensure the system (11) for $\sigma_\phi = 0$ is Hurwitz, $\gamma_{\phi 1}$ and $\gamma_{\phi 2}$ will be selected to satisfy

$$\begin{cases} \gamma_{\phi 1} \in (0, 1) \\ \gamma_{\phi 2} = \frac{2\gamma_{\phi 1}}{1+\gamma_{\phi 1}} \end{cases} \quad (12)$$

and to make the variable σ_ϕ differentiable. The notation $\text{sig}(x)^a$ as first defined in [27] is a simplified expression of

$$\text{sig}(x)^a = |x|^a \text{sgn}(x). \tag{13}$$

Note that for $a > 0, \forall x \in \mathcal{R}, \text{sig}(x)^a$ is a monotonically increasing smooth function [24].

Now, we shall derive an expression of control input based on equivalent control input method. On the sliding mode, we have

$$\dot{\sigma}_\phi = \ddot{e}_\phi + \lambda_{\phi 1}\text{sig}(e_\phi)^{\gamma_{\phi 1}} + \lambda_{\phi 2}\text{sig}(\dot{e}_\phi)^{\gamma_{\phi 2}} = 0. \tag{14}$$

Removing the uncertain terms (i.e., $\delta_\phi = 0$) in the first line of the system model (9) and substituting the first equation of (9) into (14), we can obtain the following equivalent control input τ_{x0}:

$$\tau_{x0} = -\ell_{10}[\lambda_{\phi 2}\text{sig}(\dot{e}_\phi)^{\gamma_{\phi 2}} + \lambda_{\phi 1}\text{sig}(e_\phi)^{\gamma_{\phi 1}}]$$
$$+ \ell_{30}p + \ell_{10}\ddot{\phi}_d - \ell_{20}qr. \tag{15}$$

Furthermore, we introduce a reaching control input

$$\tau_{x1} = -\ell_{10}[b_{\phi 1}\sigma_\phi + b_{\phi 2}\text{sig}(\sigma_\phi)^{\beta_\phi} + (\hat{C}_{\phi_1}$$
$$+ \hat{C}_{\phi_2}|\phi| + \hat{C}_{\phi_3}|\dot{\phi}|)\text{sgn}(\sigma_\phi)] \tag{16}$$

where $b_{\phi 1}, b_{\phi 2} > 0$, and $\beta_\phi > 0$ are the control parameters to be selected. $\hat{C}_{\phi_1}, \hat{C}_{\phi_2}$, and $\hat{C}_{\phi_3}$ are the parameter estimates related to the uncertainties, which are updated by the following adaptive estimation algorithm:

$$\dot{\hat{C}}_{\phi_1} = (1 + \frac{1}{\mu_1})|\sigma_\phi|$$

$$\dot{\hat{C}}_{\phi_2} = (1 + \frac{1}{\mu_2})|\sigma_\phi||\phi|$$

$$\dot{\hat{C}}_{\phi_3} = (1 + \frac{1}{\mu_3})|\sigma_\phi||\dot{\phi}| \tag{17}$$

with $\mu_1, \mu_2, \mu_3 > 1$ to be designed. By summing up the equivalent and reaching control inputs, the overall control input for the roll motion control can be derived as

$$\tau_x = \tau_{x0} + \tau_{x1}. \tag{18}$$

Similarly, we can design the pitch and yaw angle controller in the form of

$$\begin{cases} \tau_y = \tau_{y0} + \tau_{y1} \\ \tau_z = \tau_{z0} + \tau_{z1} \end{cases} \tag{19}$$

where

$$\tau_{y0} = -\ell_{40}[\lambda_{\theta 2}\text{sig}(\dot{e}_\theta)^{\gamma_{\theta 2}} + \lambda_{\theta 1}\text{sig}(e_\theta)^{\gamma_{\theta 1}}]$$
$$+ \ell_{60}q + \ell_{40}\ddot{\theta}_d - \ell_{50}pr \tag{20}$$

$$\tau_{y1} = -\ell_{40}[b_{\theta 1}\sigma_\theta + b_{\theta 2}\text{sig}(\sigma_\theta)^{\beta_\theta} + (\hat{C}_{\theta_1}$$
$$+ \hat{C}_{\theta_2}|\theta| + \hat{C}_{\theta_3}|\dot{\theta}|)\text{sgn}(\sigma_\theta)] \tag{21}$$

and

$$\tau_{z0} = -\ell_{70}[\lambda_{\psi 2}sig(\dot{e}_\psi)^{\gamma_{\psi 2}} + \lambda_{\psi 1}\text{sig}(e_\psi)^{\gamma_{\psi 1}}]$$
$$+ \ell_{90}r + \ell_{70}\ddot{\psi}_d - \ell_{50}pq \tag{22}$$

$$\tau_{z1} = -\ell_{70}[b_{\psi 1}\sigma_\psi + b_{\psi 2}\text{sig}(\sigma_\psi)^{\beta_\psi} + (\hat{C}_{\psi_1}$$
$$+ \hat{C}_{\psi_2}|\psi| + \hat{C}_{\psi_3}|\dot{\psi}|)\text{sgn}(\sigma_\psi)] \tag{23}$$

where the estimation adaptive law for pitch and yaw are as follows:

$$\begin{cases} \dot{\hat{C}}_{*1} = (1 + \frac{1}{\mu_1})|\sigma_*| \\ \dot{\hat{C}}_{*2} = (1 + \frac{1}{\mu_2})|\sigma_*|| * |, \quad * \in \{\theta, \psi\} \\ \dot{\hat{C}}_{*3} = (1 + \frac{1}{\mu_3})|\sigma_*||\dot{*}| \end{cases} \tag{24}$$

with the sliding mode functions for yaw and pitch motion, respectively, given by

$$\sigma_\theta = e_\theta + \int_{t_0}^t \lambda_{\theta 2}\text{sig}(\dot{e}_\theta)^{\gamma_{\theta 2}} + \lambda_{\theta 1}\text{sig}(e_\theta)^{\gamma_{\theta 1}}d\tau$$

$$\sigma_\psi = e_\psi + \int_{t_0}^t \lambda_{\psi 2}\text{sig}(\dot{e}_\psi)^{\gamma_{\psi 2}} + \lambda_{\psi 1}\text{sig}(e_\psi)^{\gamma_{\psi 1}}d\tau. \tag{25}$$

B. Stability Analysis

For stability analysis, we first introduce the following definition and lemma.

Definition 1 ([28]–[30]): Let $f(x) = (f_1(x), \ldots, f_n(x))^T$ be a continuous vector field. There exists $(r_1, r_2, \ldots, r_n) \in \mathbb{R}^n$ with $r_i > 0 \, (i = 1, \ldots, n.)$ that satisfies the following conditions of $f(x)$, if, for any given $\varepsilon > 0$:

$$f_i(\varepsilon^{r_1}x_1, \varepsilon^{r_2}x_2, \ldots, \varepsilon^{r_n}x_n) = \varepsilon^{r_i+k}f_i(x), i = 1, 2, \ldots, n \tag{26}$$

where $k \geq -\max\{r_i, i = 1, 2, \ldots, n\}$, $f(x)$ is said to be homogeneous of degree k with respect to $(r_1, r_2, \ldots, r_n)$.

Lemma 1 ([31], [32]): Suppose that a system $\dot{x} = f(x)$ satisfies $f(0) = 0$ and is homogeneous of degree $k < 0$, then the system is global finite-time stable if the system is asymptotically stable.

Now, we conclude the following theorem for the proposed AFNTSM controller.

Theorem 1: Consider the uncertain quadrotor system in (9), under the AFNTSM control law (18), and (19).

The finite-time convergence of the attitude tracking errors can be guaranteed. In addition, the following properties of the control system hold.

1) The sliding variable σ_* converges to zero from any initial conditions in the finite time

$$T_{r*} < \frac{2V_*^{\frac{1}{2}}(0)}{\mathfrak{B}} \tag{27}$$

where $\mathfrak{B}$ will be defined in (32), V_* is a Lyapunov function given in (29). Furthermore, the attitude tracking errors e_* can converge to zero in the finite time $T_{a*} = T_{\sigma*} + T_{r*}$, $* \in \{\phi, \theta, \psi\}$, where the $T_{\sigma*}$ is the time taken from sliding surface to the origin.

2) For the adaptive estimation algorithm (17), $\hat{C}_{*i}, * \in \{\phi, \theta, \psi\}$ is upper bounded, that is, there exists a positive number C_{*i} in (10) such that $\hat{C}_{*i} < C_{*i}$ always holds.

Proof: Since each attitude angle has the same control structure, we only give the stability proof for roll motion control. The

proof procedure can be applied to the yaw and pitch control as well.

First, substituting the first equation of (9) into (11), we can obtain

$$\dot{\sigma}_\phi = -[b_{\phi 1}\sigma_\phi + b_{\phi 2}\mathrm{sig}(\sigma_\phi)^{\beta_\phi} + (\hat{C}_{\phi 1} + \hat{C}_{\phi 2}|\phi| \\ + \hat{C}_{\phi 3}|\dot{\phi}|)\mathrm{sgn}(\sigma_\phi)] - \frac{1}{\ell_{10}}\delta_\phi. \qquad (28)$$

Next, define a Lyapunov function as

$$V_\phi = \frac{1}{2}\sigma_\phi^2 + \frac{1}{2}\sum_{i=1}^{3}\mu_i \tilde{C}_{\phi i}^2 \qquad (29)$$

where μ_i is a positive number and $\tilde{C}_{\phi i} = \hat{C}_{\phi i} - C_{\phi i}$ ($i = 1, 2, 3$) are the estimation biases. From (29), the time derivative of V_ϕ is

$$\dot{V}_\phi = \sigma_\phi \dot{\sigma}_\phi + \sum_{i=1}^{3}\mu_i \tilde{C}_{\phi i}\dot{\tilde{C}}_{\phi i}$$

$$= -[b_{\phi 1}\sigma_\phi^2 + b_{\phi 2}|\sigma_\phi|^{\beta_\phi+1} + (\hat{C}_{\phi 1} + \hat{C}_{\phi 2}|\phi| \\ + \hat{C}_{\phi 3}|\dot{\phi}|)|\sigma_\phi|] - \frac{1}{\ell_{10}}\delta_\phi\sigma_\phi + \sum_{i=1}^{3}\mu_i \tilde{C}_{\phi i}\dot{\tilde{C}}_{\phi i}$$

$$\leq \frac{1}{\ell_{10}}|\delta_\phi||\sigma_\phi| - (\hat{C}_{\phi 1} + \hat{C}_{\phi 2}|\phi| + \hat{C}_{\phi 3}|\dot{\phi}|)|\sigma_\phi| \\ + \sum_{i=1}^{3}\mu_i \tilde{C}_{\phi i}\dot{\tilde{C}}_{\phi i} + (C_{\phi 1} + C_{\phi 2}|\phi| \\ + C_{\phi 3}|\dot{\phi}|)|\sigma_\phi| - (C_{\phi 1} + C_{\phi 2}|\phi| + C_{\phi 3}|\dot{\phi}|)|\sigma_\phi|$$

$$= -(C_{\phi 1} + C_{\phi 2}|\phi| + C_{\phi 3}|\dot{\phi}| - \frac{1}{\ell_{10}}|\delta_\phi||\sigma_\phi|)|\sigma_\phi| \\ - (\tilde{C}_{\phi 1} + \tilde{C}_{\phi 2}|\phi| + \tilde{C}_{\phi 3}|\dot{\phi}|)|\sigma_\phi| \\ + \sum_{i=1}^{3}\mu_i \tilde{C}_{\phi i}\dot{\tilde{C}}_{\phi i}$$

$$= -(C_{\phi 1} + C_{\phi 2}|\phi| + C_{\phi 3}|\dot{\phi}| - \frac{1}{\ell_{10}}|\delta_\phi||\sigma_\phi|)|\sigma_\phi| \\ + [(\hat{C}_{\phi i} - C_{\phi i})\mu_1|\sigma_\phi| + (\hat{C}_{\phi i} \\ - C_{\phi i})\mu_2|\sigma_\phi||\phi| + (\hat{C}_{\phi i} - C_{\phi i})\mu_3|\sigma_\phi||\dot{\phi}|]. \qquad (30)$$

Suppose $\sigma_\phi \neq 0$, since the adaptive law (17) is positive, it follows that $\hat{C}_{\phi i}$ ($i = 1, 2, 3$) is increasing and there exists a time instance t_1 such that:

$$|b_{\phi 1}\sigma_\phi + b_{\phi 2}\mathrm{sig}(\sigma_\phi)^{\beta_\phi} + \frac{1}{\ell_{10}}\delta_\phi| < \hat{C}_{\phi 1} + \hat{C}_{\phi 2}|\phi| + \hat{C}_{\phi 3}|\dot{\phi}|. \qquad (31)$$

Based on (28), after $t = t_1$ the adaptive estimation algorithm starts to drive the sliding variable σ_ϕ to converge to zero. Then, the adaptive estimation value continues to increase in finite time Δt until the sliding variable $\sigma_\phi = 0$. Finally, $\hat{C}_{\phi i}$ will stay at $\hat{C}_{\phi i}(t_1 + \Delta t)$. Note that $\hat{C}_{\phi i}$ is a continuous function, which means that $\hat{C}_{\phi i}$ has an upper bound. Hence, there exists such a

positive number $C_{\phi i}$ in (10) satisfying $\hat{C}_{\phi i} < C_{\phi i}$ ($i = 1, 2, 3$) and, thus, following (30) yields:

$$\dot{V}_\phi < -\Psi_\sigma\frac{|\sigma_\phi|}{\sqrt{2}} - \Psi_1\sqrt{\frac{\mu_1}{2}}|\tilde{C}_{\phi 1}| - \Psi_2\sqrt{\frac{\mu_2}{2}}|\tilde{C}_{\phi 2}| \\ - \Psi_3\sqrt{\frac{\mu_3}{2}}|\tilde{C}_{\phi 3}|$$

$$\leq -\mathfrak{B}V_\phi^{\frac{1}{2}} \qquad (32)$$

where $\mathfrak{B} = \min(\Psi_\sigma, \Psi_1, \Psi_2, \Psi_3)$

$$\Psi_\sigma = \sqrt{2}(C_{\phi 1} + C_{\phi 2}|\phi| + C_{\phi 3}|\dot{\phi}| - \frac{1}{\ell_{10}}|\delta_\phi|)$$

$$\Psi_1 = \sqrt{2\mu_1}|\sigma_\phi|$$

$$\Psi_2 = \sqrt{2\mu_2}|\sigma_\phi||\phi|$$

$$\Psi_3 = \sqrt{2\mu_3}|\sigma_\phi||\dot{\phi}|. \qquad (33)$$

According to (10) and (33), it is obvious that $\Psi_\sigma > 0$, $\Psi_1 > 0$, $\Psi_2 > 0$, $\Psi_3 > 0$. For any initial condition $V_\phi(x(0)) = V_\phi(0)$, the function $V_\phi(x)$ can converge to the equilibrium point in finite time given by

$$\int_{V_\phi(0)}^{0} -V_\phi^{\frac{1}{2}}dV_\phi < \int_{0}^{T_{r\phi}}\mathfrak{B}dt$$

$$T_{r\phi} < \frac{2V_\phi^{\frac{1}{2}}(0)}{\mathfrak{B}}. \qquad (34)$$

Furthermore, we can prove that the attitude tracking error e_ϕ converges to zero in a finite time $T_{\phi\sigma}$ when the sliding mode function $\sigma_\phi = 0$. At the sliding surface $\sigma_\phi = 0$, (11) can be rewritten in the form as

$$\begin{aligned} \dot{x}_1 &= x_2 \\ \dot{x}_2 &= -\lambda_{\phi 2}\mathrm{sig}(x_2)^{\gamma_{\phi 2}} - \lambda_{\phi 1}\mathrm{sig}(x_1)^{\gamma_{\phi 1}} \end{aligned} \qquad (35)$$

where $x_1 = e_\phi$ and $x_2 = \dot{e}_\phi$. Define the Lyapunov function as

$$V_{\phi\sigma} = \frac{\lambda_{\phi 1}}{\gamma_{\phi 1} + 1}|x_1|^{\gamma_{\phi 1}+1} + \frac{1}{2}|x_2|^2 \qquad (36)$$

whose time derivative can be obtained as

$$\dot{V}_{\phi\sigma} = -\lambda_{\phi 2}|x_2|^{\gamma_{\phi 2}+1} \leq 0 \qquad (37)$$

implying that $V_{\phi\sigma}$ is a monotonically nonincreasing function and has a finite bound, so the system (35) is asymptotically stable.

Based on Definition 1, substituting (35) into (26) yields

$$\begin{aligned} f_1(\varepsilon^{\alpha_1}x_1, \varepsilon^{\alpha_2}x_2) &= \varepsilon^{\alpha_1+k}x_2 \\ f_2(\varepsilon^{\alpha_1}x_1, \varepsilon^{\alpha_2}x_2) &= [-\lambda_{\phi 2}\mathrm{sig}(x_2)^{\gamma_{\phi 2}} \\ &\quad - \lambda_{\phi 1}\mathrm{sig}(x_1)^{\gamma_{\phi 1}}]\varepsilon^{\alpha_2+k}. \end{aligned} \qquad (38)$$

According to (12) and (38), we have

$$\begin{cases} \alpha_2 = \alpha_1 + k \\ \alpha_2\gamma_{\phi 2} = \alpha_1\gamma_{\phi 1} = k + \alpha_2 \\ \gamma_{\phi 2} = \frac{2\gamma_{\phi 1}}{1+\gamma_{\phi 1}} \end{cases}. \qquad (39)$$

By calculating the array equation mentioned above, it gives

$$\begin{cases} k = \frac{\gamma_{\phi 1}-1}{2}\alpha_1 \geq -\max\{\alpha_1,\alpha_2\} \\ \alpha_2 = \frac{\gamma_{\phi 1}-1}{2}\alpha_1 \\ \alpha_1 = \alpha_1 \end{cases}. \qquad (40)$$

Let $\alpha_1 = 1$, $\alpha_2 = \frac{(1+\gamma_{\phi 1})}{2}$, $k = \frac{\gamma_{\phi 1}-1}{2}$, and $\gamma_{\phi 1} \in (0,1)$, so we have $k = \frac{\gamma_{\phi 1}-1}{2} < 0$. According to Lemma 1, the system (35) is global finite-time stable.

For the system (35), there exists a time instance t_s such that $\ddot{e}_\phi(t) = 0$ for $t \geq t_s$ and, therefore, the first derivative of σ_ϕ in (11) is reduced to

$$\lambda_{\phi 2}\mathrm{sig}(\dot{e}_\phi)^{\gamma_{\phi 2}} + \lambda_{\phi 1}\mathrm{sig}(e_\phi)^{\gamma_{\phi 1}} = 0. \qquad (41)$$

According to [20], it can be inferred that (41) for the tracking error $e_\phi(t_s)$ can converge to zero in a finite time t_r bounded by

$$\begin{aligned} t_r &= \int_0^{|e_\phi(0)|} \left(\frac{\lambda_{\phi 2}}{\lambda_{\phi 1}}\right)^{\frac{\gamma_{\phi 1}+1}{2\gamma_{\phi 1}}} \left(\frac{1}{e_\phi^{\gamma_{\phi 1}}}\right)^{\frac{\gamma_{\phi 1}+1}{2\gamma_{\phi 1}}} de_\phi \\ &= \frac{2}{1-\gamma_{\phi 1}}\left(\frac{\lambda_{\phi 2}}{\lambda_{\phi 1}}\right)^{\frac{\gamma_{\phi 1}+1}{2\gamma_{\phi 1}}} |e_\phi(0)|^{\frac{1-\gamma_{\phi 1}}{2}}. \end{aligned} \qquad (42)$$

Hence, when $\sigma_\phi = 0$ in (11), any initial condition $e_\phi(0)$ converges to zero in a finite time $T_{\sigma\phi} = t_s + t_r$.

By following a similar procedure, the stability proof of pitch and yaw motion can be also achieved. ∎

Remark 1: Compared to the CSM [19] or TSM [15], the AFNTSM is featured with the integral element for eliminating the static deviation of attitude tracking, as shown in (11). It can also enforce the system error to converge to zero swiftly in the global space by using the term $\lambda_{\phi 2}sig(\dot{e}_\phi)^{\gamma_{\phi 2}} + \lambda_{\phi 1}sig(e_\phi)^{\gamma_{\phi 1}}$ in (11) to dominate the control when the system error is far away from the origin whilst by using the term $\dot{e}_\phi$ in (11) to dominate the control when the system error is near the origin. Compared to the FNTSM [24], the proposed AFNTSM enhances the tracking errors to be able to finite-time converge to zero instead of a bounded region.

Remark 2: In practical applications, the sliding mode variable σ_ϕ will inevitably encounter chattering due to measurement noises, which gives rise to overly large estimation of C_{*i}, as can be seen from (17) and (24). To alleviate this problem, the dead zone technique [12] can be used to alter the adaptive law as follows:

$$\begin{aligned} \dot{\hat{C}}_{\phi 1} &= \begin{cases} (1+\frac{1}{\mu_1})|\sigma_\phi|, & \text{for } |\sigma_\phi| \leq \epsilon \\ 0, & \text{for } |\sigma_\phi| > \epsilon \end{cases} \\ \dot{\hat{C}}_{\phi 2} &= \begin{cases} (1+\frac{1}{\mu_2})|\sigma_\phi||\phi|, & \text{for } |\sigma_\phi| > \epsilon \\ 0, & \text{for } |\sigma_\phi| \leq \epsilon \end{cases} \\ \dot{\hat{C}}_{\phi 3} &= \begin{cases} (1+\frac{1}{\mu_3})|\sigma_\phi||\dot{\phi}|, & \text{for } |\sigma_\phi| > \epsilon \\ 0, & \text{for } |\sigma_\phi| \leq \epsilon \end{cases} \end{aligned} \qquad (43)$$

where $\epsilon > 0$ represents a threshold of the deviation value due to the affecting factors, such as the sensor noises, the uncertainty of the estimator, and the inertial delay of the motors (e.g., $\epsilon = 0.5$ in our case). It is obvious that when sliding variable converges to the threshold, $\hat{C}_{\phi 1}$, $\hat{C}_{\phi 2}$, and $\hat{C}_{\phi 3}$ will not increase but retain their present values. It can be easily proved that for $|\sigma_\phi| \leq \epsilon$, (32) holds and, therefore, Theorem 1 is valid as well.
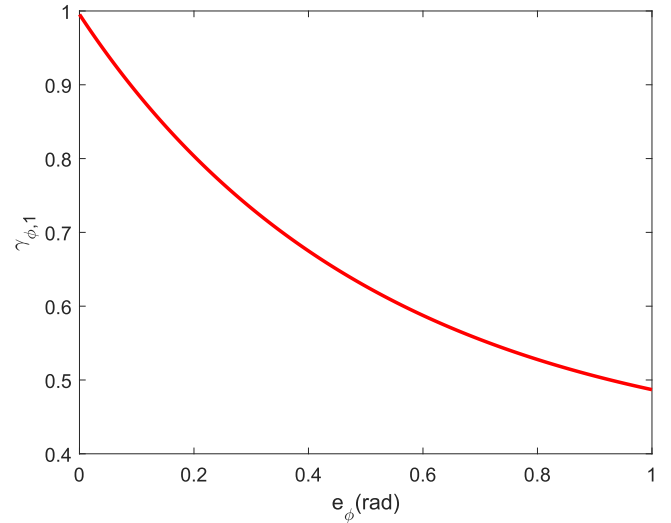

Fig. 2. Empirical function for $\gamma_{\phi 1}$ with respect to roll angle tracking error.

C. Control Parameters Selection

In practical applications, the tracking performance of quadrotor attitude control will be affected by several factors including control input saturation, input command smoothness, and sensor noises. It is also recognized that the performance specifications have to be compromised with respect to the control parameters. Hence, we shall discuss the selection guideline of the AFNTSM controller parameters with the roll angle controller taken as an illustrative example.

1) Selection of $\gamma_{\phi 1}$: $\gamma_{\phi 1} \in (0,1)$ dominates the attitude tracking error in the sliding mode function σ_ϕ, as shown in (11). A small value of $\gamma_{\phi 1}$ can increase the response speed but reversely cause excessive chattering, and even make the system divergent. To moderate this problem, we provide an empirical function as follows:

$$\gamma_{\phi 1} = \exp[-(|e_\phi|+0.23)^{1.2} - (|e_\phi|+0.23)^{0.72}] + 0.4. \qquad (44)$$

Instead of using a fixed $\gamma_{\phi 1}$, we propose the above $\gamma_{\phi 1}$ as a function that is monotonically decreasing with respect to the tracking error ϕ, as can be seen from Fig. 2. The purpose is to ensure the response speed meanwhile reduce the chattering when the error is small. One can easily verify that when the above $\gamma_{\phi 1}$ function is used in the controller, (37) still holds.

2) Selections of $\lambda_{\phi 1}$, $\lambda_{\phi 2}$: The integral gains determine the returned value of the integral element in the sliding mode variable σ_ϕ in (11). According to (42), the finite time $T_{\phi\sigma}$ is inversely proportional to $\lambda_{\phi 1}$ and directly proportional to $\lambda_{\phi 2}$. A larger $\lambda_{\phi 1}$ can increase the convergence rate of σ_ϕ as well as the amplitude of the integral element in (11), but it may also cause severe chattering. Similarly, a smaller $\lambda_{\phi 2}$ reduces the convergence time but leads to smaller overshoot. We choose $\lambda_{\phi 1} = 27$, $\lambda_{\phi 2} = 5.5$.

3) Selections of β_ϕ, $b_{\phi 1}$, $b_{\phi 2}$: The parameter β_ϕ in the reaching control law (16) is designed to adjust the convergence performance of the attitude control. A larger β_ϕ increases the
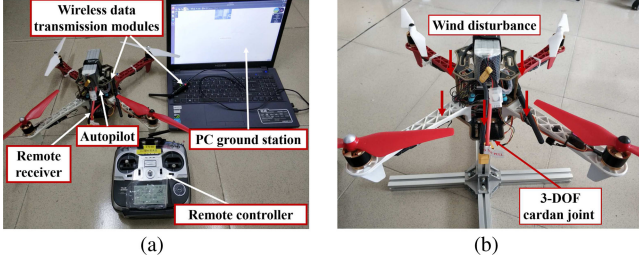
Fig. 3. Quadrotor platform used in the experiments.

response speed of the system but also introduces extra control chattering. The positive gains $b_{\phi 1}$ and $b_{\phi 2}$ affect the control signal smoothness and, thus, the level of robustness. Large $b_{\phi 1}$ and $b_{\phi 2}$ reduce the chattering but increase control input amplitude. Here, we choose $\beta_\phi = 1.63$, $b_{\phi 1} = 2.5$, and $b_{\phi 2} = 2.2$.

4) Selections of μ_1, μ_2, μ_3: The adaptation gains μ_1, μ_2, and μ_3 in (17) can be chosen sufficiently large for fast convergence to the estimated variables but not resulting in overly estimated upper bound of the system uncertainties and disturbance, which may cause actuator saturation. During the experiments, we select $\mu_1 = 20$, $\mu_2 = 20$, and $\mu_3 = 20$.

IV. EXPERIMENTAL RESULTS

Experiments are carried out on a real quadrotor to demonstrate the improved performance of the proposed controller for attitude control.[1] The quadrotor experimental platform is shown in Fig. 3(a), which consists of a PC ground station installing QGroundControl v4.0.10 software to detect quadrotor status, two wireless data transmission modules (915 MHz, 500 mW), a remote controller (Futaba, T14FG), an Autopilot with pixhawk (FMUv5) microcontroller to run the controller, and a frame with four power units (DJI F450). The sampling frequency for the controllers is 1000 Hz, which is synchronized to the angular velocity.

To obtain the values of the aerodynamic coefficients k_t and k_d in (3), the force and torque variations of the rotor with respect to its spinning rate are tested. Then, by fitting the experimental data, as shown in Fig. 4, it is found that the simulated data with $k_t = 0.0722$ and $k_d = 0.0064$ has well matched the experimental one.

A. Attitude Tracking Control Under AFNTSM

Outdoor flight experiments are conducted to test the attitude tracking control performance under the AFNTSM controller. The reference signal is generated by remote controller. The experiment results of the outdoor flight under natural wind disturbances are shown in Figs. 5–7. As shown in Fig. 5, the quadrotor attitude can quickly converge to the reference signal, which verifies the feasibility of the AFNTSM controller. Explicitly, the root-mean-square value (rms$_e$) of the attitude errors is $[0.4349°, 0.3677°, 1.3695°]$, and its maximal value (MAX$_e$) is $[1.6629°, 1.9043°, 4.2307°]$ according to the results in Fig. 6. It can be also seen that the yaw angle tracking error is larger than

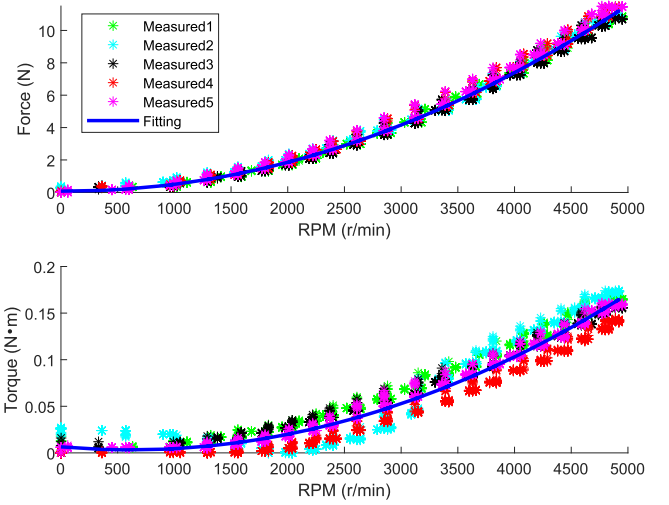[1]A demo video is [Online]. Available: https://youtu.be/avv4lW95O0k

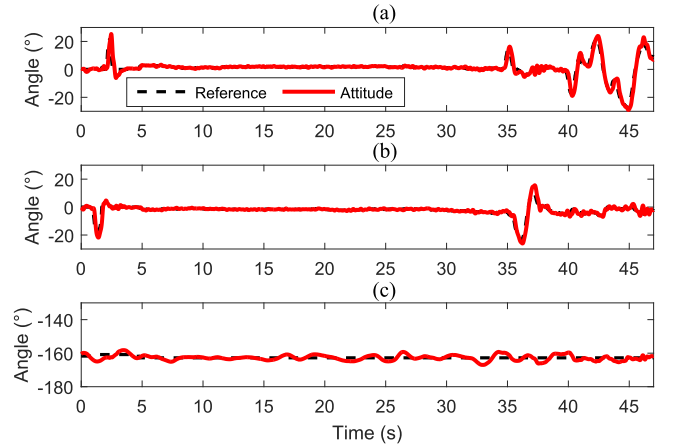Fig. 4. Curve fitting for rotor model parameters k_t and k_d.

Fig. 5. Attitude tracking responses under AFNTSM.

the others. The reason is that the aerodynamic coefficient k_d is much smaller than k_t, which means that the yaw motion is less sensitive to the rotors spinning rate as implied by (3). Fig. 7 depicts the control input commands that are feasible without significant chattering for the rotors to implement.

B. Comparative Studies

To verify the improved performance of the proposed AFNTSM, we also compare it with the recent FNTSM [24] and the CSM controller through experimental study. The equivalent control inputs of the two controllers are of the same form as AFNTSM for fair comparisons. The reaching control input of FNTSM controller is $\tau_{*\mathrm{dis}} = -\ell_{*0}[k_{*1}\sigma_* + k_{*2}\mathrm{sig}(\sigma_*)^{\rho_*}]$, where the sliding variable is in the form of $\sigma_* = e_* + \lambda_*\mathrm{sig}(\dot{e}_*)^{\beta_*}$. The reaching control input of the CSM controller is $\tau_{*\mathrm{dis}} = -\ell_{*0}[k_{*1}\sigma_* + k_{*2}\mathrm{sgn}(\sigma_*)]$ with the sliding variable in the form of $\sigma_* = e_* + \lambda_*\dot{e}$. The control parameters used in the experiment are listed in Table I.
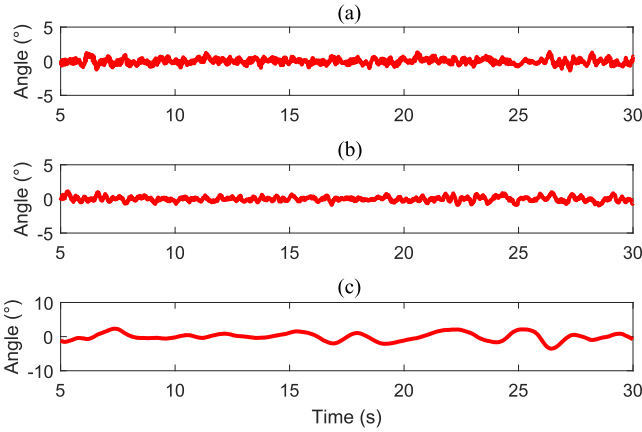
Fig. 6.   Attitude tracking errors under AFNTSM.

TABLE I
CONTROL PARAMETERS IN THE EXPERIMENTS

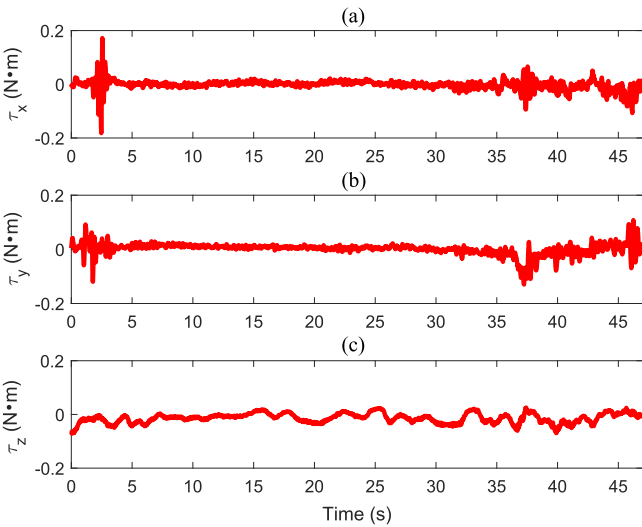| Controllers	Control parameters	Roll	Pitch	Yaw
AFNTSM	β	1.63	1.63	1.10
	λ_1	27	27	4.5
	λ_2	5.5	5.5	1.5
	b_1	2.5	2.5	2.7
	b_2	2.2	2.2	1.3
	μ_1	20	20	20
	μ_2	20	20	20
	μ_3	20	20	20
FNTSM	β	1.3	1.3	1.3
	λ	0.16	0.16	0.16
	ρ	0.6	0.6	0.6
	k_1	1.2	1.2	1.2
	k_2	20	20	20
CSM	λ	3	3	3
	k_1	8	8	8
	k_2	0.01	0.01	0.01

Fig. 7.   Control input responses under AFNTSM.

1) Case 1. Attitude Step Tracking Test: In this case, we use an indoor 3-DOF experimental platform to verify the improved robustness of the proposed AFNTSM controller, as shown in Fig. 3(b). The reference input is a step signal generated by the remote controller and the attitude tracking responses are shown in the Figs. 8– 10. The step signals are generated by setting two switches on the remote controller, respectively. The roll and pitch reference signals are generated by a three-stage switch. The yaw one is generated by the other two-stage switch. Fig. 8 shows the attitude under the AFNTSM controller converges faster to the reference signal, where the settling time of roll and pitch angle are 1.26 and 0.84 s, respectively. In addition, the AFNTSM controller achieves much smaller steady-state tracking errors as compared to that under FNTSM, as shown in Fig. 9. This is because FNTSM only ensures the tracking error to converge to a region instead of the origin.

2) Case 2. Disturbance Rejection Test: To verify the disturbance rejection performance of the three controllers, persistent wind disturbance artificially generated by a fan with a speed of 10 m/s is imposed on the quadrotor from 4 s onwards [see Fig. 3(b)]. The generated wind is moved clockwise to simulate
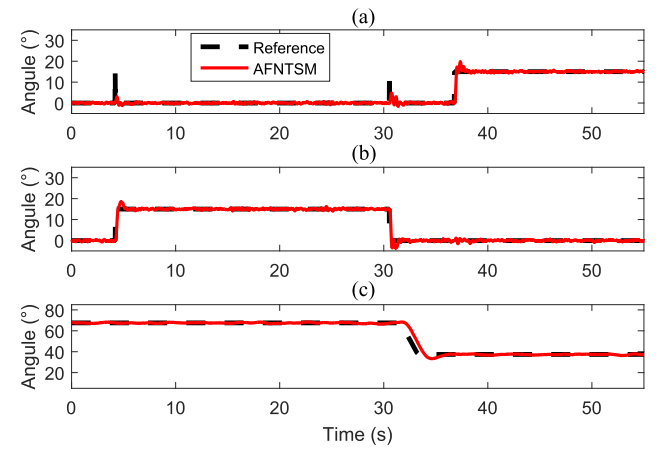

Fig. 8.   Attitude tracking responses to a step reference under AFNTSM.
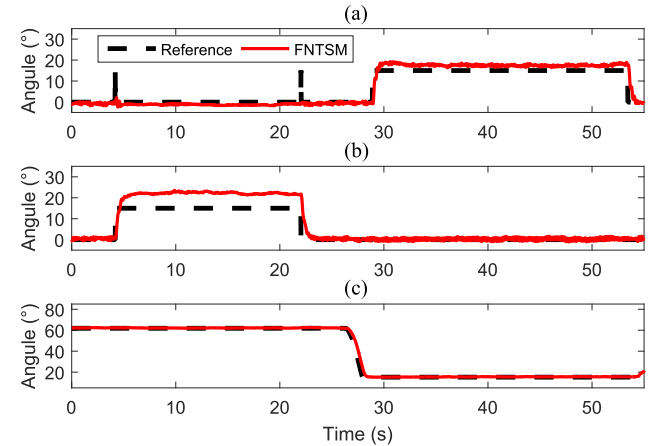
Fig. 9.   Attitude tracking responses to a step reference under FNTSM.

the uncertain wind disturbance in nature. The comparison of attitude tracking responses under the controllers are shown in Fig. 11. It is clear that the attitude of the AFNTSM controller is stabilized over the whole experimental time. This is because the adaptive control gain in (37) and (42) can adaptively approximate the upper bound of the unknown external disturbance.
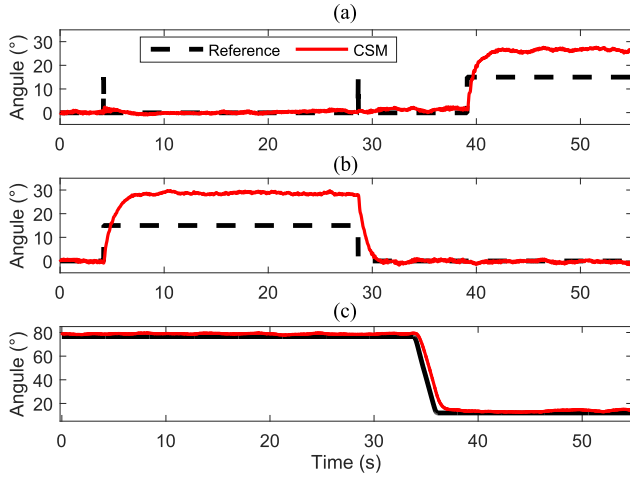
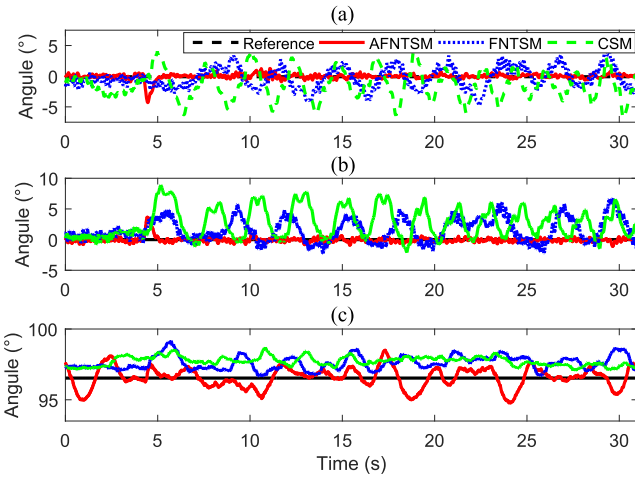Fig. 10.   Attitude tracking responses to a step reference under CSM.

Fig. 11.   Comparison of attitude tracking responses to wind disturbances.

TABLE II
SUMMARY AND COMPARISON OF CONTROL PERFORMANCE

Attitude	Controllers	Case 1			Case 2	
		Settling time (s)	RMS_e (°)	MAX_e (°)	RMS_e (°)	MAX_e (°)
Roll	AFNTSM	1.3	0.23	0.73	0.49	4.31
	FNTSM	2.5	2.87	15.92	1.69	4.70
	CSM	4.4	11.01	13.87	2.68	6.88
Pitch	AFNTSM	0.8	0.28	1.24	0.46	3.73
	FNTSM	2.5	7.12	14.40	2.42	6.69
	CSM	4.3	13.12	15.71	3.61	8.89
Yaw	AFNTSM	1.9	0.39	1.20	0.71	1.96
	FNTSM	2.4	0.36	0.88	1.17	2.64
	CSM	2.7	2.37	3.08	1.24	2.18

However, in the FNTSM and CSM controllers, the inherent fixed control gain cannot adapt to the unknown disturbance when the disturbance amplitude is larger than the fixed control gain and as a result, the tracking error is not guaranteed. The experimental results are summarized and compared in Table II.

V. CONCLUSION

In this article, an AFNTSM controller was developed for robustly fast and accurate attitude tracking control of a quadrotor. The integral element in the proposed AFNTSM controller can guarantee the attitude tracking error to converge to zero in a finite time. In addition, the proposed adaptive law can estimate the unknown disturbances online such that the disturbance rejection performance is improved and the control chattering is significantly moderated. Thanks to the proposed method, the attitude tracking error can converge to zero in a finite time and the requirement for the disturbance upper bound is removed from the controller parameters that is a practical benefit to many applications. Finally, experiments conducted on a real quadrotor platform demonstrate the advantages of higher tracking accuracy, faster response, and stronger disturbance rejection performance of the proposed AFNTSM controller compared to the FNTSM and CSM controllers.

Based on the proposed controller, the quadrotor cannot perform full attitude flight due to the problem of Gimbal lock of Euler angle. Therefore, our future work will explore the solution to overcome this problem and, thus, achieve full attitude flight performance. In addition, we will further develop novel adaptive reaching law for stronger uncertainty and disturbance compensation such that more precise aggressive flight could be achieved.

REFERENCES

[1] J. J. Roldán, G. Joossen, D. Sanz, J. D. Cerro, and A. Barrientos, "Mini-UAV based sensory system for measuring environmental variables in greenhouses," *Sensors*, vol. 15, no. 2, pp. 3334–3350, Feb. 2015.

[2] K. Guo *et al.*, "Ultra-wideband-based localization for quadcopter navigation," *Unmanned Syst.*, vol. 4, no. 1, pp. 23–34, 2016.

[3] J. Hu, J. Xu, and L. Xie, "Cooperative search and exploration in robotic networks," *Unmanned Syst.*, vol. 1, no. 1, pp. 121–142, 2013.

[4] L. F. Luque-Vega, B. Castillo-Toledo, A. Loukianov, and L. E. Gonzalez-Jimenez, "Power line inspection via an unmanned aerial system based on the quadrotor helicopter," in *Proc. IEEE Mediterranean Electrotechnical Conf.*, May 2014, pp. 393–397.

[5] Z. He *et al.*, "Fuzzy intelligent control method for improving flight attitude stability of plant protection quadrotor UAV," *Int. J. Agricultural Biol. Eng.*, vol. 12, no. 6, pp. 110–115, 2019.

[6] D. Mihailescu-Stoica, R. Acuna, and J. Adamy, "High performance adaptive attitude control of a quadrotor," in *Proc. Eur. Control Conf.*, Aug. 2019, pp. 3462–3469.

[7] Q. Tao, T. J. Tan, J. Cha, Y. Yuan, and F. Zhang, "Modeling and control of swing oscillation of underactuated indoor miniature autonomous blimps," *Unmanned Syst.*, vol. 9, no. 1, pp. 73–86, 2021.

[8] J.-J. Xiong and G.-B. Zhang, "Global fast dynamic terminal sliding mode control for a quadrotor UAV," *ISA Trans.*, vol. 66, pp. 233–240, Jan. 2017.

[9] D. Lee, H. J. Kim, and S. Sastry, "Feedback linearization vs. adaptive sliding mode control for a quadrotor helicopter," *Int. J. Control Autom. Syst.*, vol. 7, no. 3, pp. 419–428, May 2009.

[10] A. Noormohammadi-Asl, O. Esrafilian, M. A. Arzati, and H. D. Taghirad, "System identification and H$_\infty$-based control of quadrotor attitude," *Mech. Syst. Signal Process.*, vol. 135, Jan. 2020, Art. no. 106358.

[11] M. Kahouadji, M. R. Mokhtari, A. Choukchou-Braham, and B. Cherki, "Real-time attitude control of 3 dof quadrotor UAV using modified super twisting algorithm," *J. Franklin Inst.*, vol. 357, no. 5, pp. 2681–2695, Mar. 2020.

[12] C. Edwards and S. Spurgeon, *Sliding Mode Control: Theory and Applications*. Boca Raton, FL, USA: CRC Press, 1998.

[13] Z. Jia, J. Yu, Y. Mei, Y. Chen, Y. Shen, and X. Ai, "Integral backstepping sliding mode control for quadrotor helicopter under external uncertain disturbances," *Aerosp. Sci. Technol.*, vol. 68, pp. 299–307, Sep. 2017.

[14] J. C. Monteiro, F. Lizarralde, and L. Hsu, "Optimal control allocation of quadrotor UAVs subject to actuator constraints," in *Proc. Amer. Control Conf.*, Aug. 2016, pp. 500–505.

[15] S. Yu, X. Yu, B. Shirinzadeh, and Z. Man, "Continuous finite-time control for robotic manipulators with terminal sliding mode," *Automatica*, vol. 41, no. 11, pp. 1957–1964, Nov. 2005.

[16] K. Shao, J. Zheng, K. Huang, H. Wang, Z. Man, and M. Fu, "Finite-time control of a linear motor positioner using adaptive recursive terminal sliding mode," *IEEE Trans. Ind. Electron.*, vol. 67, no. 8, pp. 6659–6668, Aug. 2019.

[17] R. Cui, L. Chen, C. Yang, and M. Chen, "Extended state observer-based integral sliding mode control for an underwater robot with unknown disturbances and uncertain nonlinearities," *IEEE Trans. Ind. Electron.*, vol. 64, no. 8, pp. 6785–6795, Apr. 2017.

[18] N. Fethalla, M. Saad, H. Michalska, and J. Ghommam, "Robust observer-based dynamic sliding mode controller for a quadrotor UAV," *IEEE Access*, vol. 6, pp. 45 846–45859, Aug. 2018.

[19] R. Xu and Ü. Özgüner, "Sliding mode control of a class of underactuated systems," *Automatica*, vol. 44, no. 1, pp. 233–241, Jan. 2008.

[20] L. Yang and J. Yang, "Nonsingular fast terminal sliding-mode control for nonlinear dynamical systems," *Int. J. Robust Nonlinear Control*, vol. 21, no. 16, pp. 1865–1879, 2011.

[21] E.-H. Zheng, J.-J. Xiong, and J.-L. Luo, "Second order sliding mode control for a quadrotor UAV," *ISA Trans.*, vol. 53, no. 4, pp. 1350–1356, Jul. 2014.

[22] M. Vahdanipour and M. Khodabandeh, "Adaptive fractional order sliding mode control for a quadrotor with a varying load," *Aerosp. Sci. Technol.*, vol. 86, pp. 737–747, Mar. 2019.

[23] O. Mofid and S. Mobayen, "Adaptive sliding mode control for finite-time stability of quad-rotor UAVs with parametric uncertainties," *ISA Trans.*, vol. 72, pp. 1–14, Jan. 2018.

[24] J. Zheng, H. Wang, Z. Man, J. Jin, and M. Fu, "Robust motion control of a linear motor positioner using fast nonsingular terminal sliding mode," *IEEE/ASME Trans. Mechatronics*, vol. 20, no. 4, pp. 1743–1752, Sep. 2014.

[25] K. Shao, J. Zheng, H. Wang, F. Xu, X. Wang, and B. Liang, "Recursive sliding mode control with adaptive disturbance observer for a linear motor positioner," *Mech. Syst. Signal Process.*, vol. 146, Jan. 2020, Art. no. 107014.

[26] C.-S. Chiu, "Derivative and integral terminal sliding mode control for a class of mimo nonlinear systems," *Automatica*, vol. 48, no. 2, pp. 316–326, Feb. 2012.

[27] V. T. Haimo, "Finite time controllers," *SIAM J. Control Optim.*, vol. 24, no. 4, pp. 760–770, 1986.

[28] S. P. Bhat and D. S. Bernstein, "Continuous finite-time stabilization of the translational and rotational double integrators," *IEEE Trans. Autom. Control*, vol. 43, no. 5, pp. 678–682, May 1998.

[29] Y. Hong, J. Huang, and Y. Xu, "On an output feedback finite-time stabilization problem," *IEEE Trans. Autom. Control*, vol. 46, no. 2, pp. 305–309, Feb. 2001.

[30] L. Rosier, "Homogeneous lyapunov function for homogeneous continuous vector field," *Syst. Control Lett.*, vol. 19, no. 6, pp. 467–473, Dec. 1992.

[31] S. P. Bhat and D. S. Bernstein, "Finite-time stability of homogeneous systems," in *Proc. Amer. Control Conf.*, vol. 4, Jun. 1997, pp. 2513–2514.

[32] Y. Hong, Y. Xu, and J. Huang, "Finite-time control for robot manipulators," *Syst. Control Lett.*, vol. 46, no. 4, pp. 243–253, Jul. 2002.

Wei Meng (Member, IEEE) received the B.E. and M.E. degrees from Northeastern University, Shenyang, China, in 2006 and 2008, respectively, both in electrical engineering, and the Ph.D. degree in control and instrumentation from the Nanyang Technological University, Singapore, in 2013.

From 2012 to 2017, he was a Research Scientist with UAV Research Group, Temasek Laboratories, National University of Singapore. He is currently with the School of Automation, Guangdong University of Technology as a Professor. His current research interests include unmanned systems, cooperative control, multirobot systems, localization, and tracking.
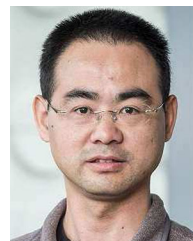
Zemin Lin received the B.S. degree in aircraft design and engineering from the School of Aeronautical Engineering from the Zhengzhou University of Aeronautics, Zhengzhou, China, in 2017. He is currently working toward the M.Eng. degree in control engineering with the School of Automation, Guangdong University of Technology, Guangzhou, China.

His research interests include sliding mode control, tiltrotor aircraft, and learning algorithms.

Ke Shao received the B.E. and Ph.D. degrees from the School of Mechanical Engineering, Hefei University of Technology, Hefei, China, in 2013 and 2019, respectively, both in mechanical engineering.

From 2017 to 2019, he was a Visiting Scholar with the School of Software and Electrical Engineering, Swinburne University of Technology, Melbourne, Australia, founded by China Scholarship Council. Currently, he is the Postdoc Research Fellow with Tsinghua Shenzhen International Graduate School, Tsinghua University, Shenzhen, China. His research interests include mechanical system dynamics, sliding mode control, advanced robots, high-precision motion control, and vehicle dynamics and control.

Shikang Lian received the B.S. degree in automation from the School of Automation, Zhongkai University of Agriculture and Engineering, Guangzhou, China, in 2018. He is currently working toward the Ph.D. degree in control science and engineering with the School of Automation, Guangdong University of Technology, Guangzhou, China.

His research interests include adaptive control, sliding mode control, unmanned aerial vehicle design, high-precision motion control, and learning algorithms.

Jinchuan Zheng (Senior Member, IEEE) received the B.Eng. and M.Eng. degrees in mechatronics engineering from Shanghai Jiao Tong University, Shanghai, China, in 1999 and 2002, respectively, and the Ph.D. degree in electrical and electronic engineering from Nanyang Technological University, Singapore, in 2006.

In 2005, he was with the Australian Research Council Centre of Excellence for Complex Dynamic Systems and Control, School of Electrical and Computer Engineering, University of Newcastle, Callaghan, NSW, Australia, as a Research Academic. From 2011 to 2012, he was a Staff Engineer with the Western Digital Hard Disk Drive R&D Center, Singapore. Since 2012, he has been with Swinburne University of Technology, Melbourne, VIC, Australia. He is currently an Associate Professor with the Faculty of Science, Engineering and Technology. His research interests include high precision motion control systems, electric vehicle control technology, mobile robots, and biomechatronic devices.

Hongyi Li (Senior Member, IEEE) received the Ph.D. degree in intelligent control from the University of Portsmouth, Portsmouth, U.K., in 2012.

He was a Research Associate with the Department of Mechanical Engineering, University of Hong Kong, Hong Kong and Hong Kong Polytechnic University, Hong Kong. He was a Visiting Principal Fellow with the Faculty of Engineering and Information Sciences, University of Wollongong, Wollongong, Australia. He is currently a Professor with the Guangdong University of Technology, Guangdong, China. His research interests include intelligent control, cooperative control, sliding mode control, and their applications.

Prof. Li was a recipient of the 2016 and 2019 Andrew P. Sage Best Transactions Paper Awards from IEEE System, Man, Cybernetics Society, the Best Paper Award in Theory from ICCSS 2017 and the Zadeh Best Student Paper from IEEE ICCSS 2019, respectively. He has been with the editorial board of several international journals, including IEEE TRANSACTIONS ON NEURAL NETWORKS AND LEARNING SYSTEMS, IEEE TRANSACTIONS ON FUZZY SYSTEMS, IEEE TRANSACTIONS ON SYSTEMS, MAN AND CYBERNETICS: SYSTEMS, IEEE TRANSACTIONS ON COGNITIVE AND DEVELOPMENTAL SYSTEMS, *SCIENCE CHINA Information Sciences*, IEEE/CAA JOURNAL OF AUTOMATICA SINICA, *Journal of Systems Science and Complexity*, *Neural Networks*, *Asian Journal of Control, Circuits, Systems and Signal Processing*, and *International Journal of Control, Automation and Systems*. He has been Guest Editors of the IEEE TRANSACTIONS ON CYBERNETICS and *IET Control Theory and Applications*. He is a member of the IFAC Technical Committee on Computational Intelligence in Control.

Renquan Lu (Senior Member, IEEE) received the Ph.D. degree in control science and engineering from Zhejiang University, Hangzhou, China, in 2004.

He is currently a Professor with the School of Automation, Guangdong University of Technology, Guangzhou, China. His research was supported by the National Science Fund for Distinguished Young Scientists of China in 2014, honored as the Distinguished Professor of Pearl River Scholars Program of Guangdong Province in 2015, and the Yangtze River Scholars Program by the Ministry of Education of China in 2017. His current research interests include complex systems, networked control systems, and nonlinear systems.